Journal of Colloid and Interface Science 351 (2010) 122–127

Contents lists available at ScienceDirect

Journal of Colloid and Interface Science

www.elsevier.com/locate/jcis

Folding/aggregation of graphene oxide and its application in Cu^{2+} removal

Sheng-Tao Yang [a,b], Yanli Chang [a], Haifang Wang [a,*], Gangbo Liu [a], Sheng Chen [a], Yanwen Wang [a], Yuanfang Liu [a,b], Aoneng Cao [a]

[a] Institute of Nanochemistry and Nanobiology, Shanghai University, Shanghai 200444, China
[b] Beijing National Laboratory of Molecular Science, College of Chemistry and Molecular Engineering, Peking University, Beijing 100871, China

ARTICLE INFO

Article history:
Received 28 May 2010
Accepted 18 July 2010
Available online 23 July 2010

Keywords:
Graphene oxide
Copper ions
Aggregation
Absorption
Decontamination

ABSTRACT

Graphene oxide (GO) can be aggregated by Cu^{2+} in aqueous solution with a huge Cu^{2+} absorption capacity. The Cu^{2+} causes GO sheets to be folded and also to form large aggregates that were characterized by confocal microscopy and atomic force microscopy. The folding/aggregation is most likely triggered by the coordination between GO and Cu^{2+}. The equilibrium Cu^{2+} concentrations and equilibrium absorption capacity of GO were measured to estimate the maximum absorption capacity of GO for Cu^{2+} and the absorption model. GO has a huge absorption capacity for Cu^{2+}, which is around 10 times of that of active carbon. Representative results are presented and the implication to Cu^{2+} removal is discussed.

1. Introduction

Since the discovery, graphene has attracted tremendous research interest for its potential applications [1,2]. Yet, more applications are expected to be developed along with a better understanding of the fundamental properties of graphene and its derivatives. Previous studies have explored the chemical, mechanical, optical and electronic properties of graphene and its derivatives [1–4]. Recently, it is found that graphene can be folded and aggregated under different conditions [5–7].

Among the graphene derivatives, graphene oxide (GO) is of prime importance and has been extensively studied, because GO can be chemically reduced to generate bulk amount of graphene [8]. Single-layer graphene sheet-based composites can also be synthesized directly from GO in an easy one-pot reaction [9]. GO also has many other potential applications [10–15].

Chemically, GO has plenty of oxygen atoms on the graphitic backbone in the forms of epoxy, hydroxyl, and carboxyl groups [16]. These oxygen groups can bind to metal ions, especially the multivalent metal ions [17,18], through both electrostatic and coordinate approaches. Herein, we report that the interaction of GO with Cu^{2+} in the aqueous solution leads to the folding and aggregation of GO. The morphology of the aggregates is characterized by confocal microscopy, atomic force microscopy (AFM), scanning electron microscopy (SEM) and transmission electron microscopy (TEM). The absorption capacity of GO for Cu^{2+} is measured and the absorption model is investigated. The implication of using graphene as Cu^{2+} absorbent is discussed.

* Corresponding author. Fax: +86 21 66135275.
E-mail address: hwang@shu.edu.cn (H. Wang).

0021-9797/$ - see front matter © 2010 Elsevier Inc. All rights reserved.
doi:10.1016/j.jcis.2010.07.042

2. Materials and methods

2.1. Preparation of GO

GO was prepared following the modified Hummers method [9,19,20]. Briefly, a mixture of graphite (3.0 g), $K_2S_2O_8$ (2.5 g) and P_2O_5 (2.5 g) was added into 12 mL of H_2SO_4 and stirred at 80 °C for 4.5 h. After cooling to room temperature, the suspension was diluted with 500 mL deionized water and then filtered with a filter (pore size: 0.45 μm). The filter cake was washed with deionized water to remove impurities and excess acid (near neutral) and dried under vacuum at 80 °C. The residue was collected and added into 120 mL of H_2SO_4. Then, $KMnO_4$ (15 g) was added slowly while vigorous stirring. The reaction was carried through at 35 °C for 2 h. Next, with the addition of 250 mL deionized water, the mixture was stirred for another 2 h. To the mixture, 500 mL deionzed water and 20 mL H_2O_2 (30% v/v) were added. After filtration, the residue was washed by HCl (10% v/v) and deionized water in turn, dialyzed against deionized water for 7 days, dispersed in water (0.1 mg/mL) and sonicated (40 kHz, 50 W) for 30 min to generate single-layered GO [9]. The obtained GO was characterized by infrared spectrum (IR, Avatar 370, Thermo Nicolet, USA), X-ray photoelectron spectrum (XPS, Kratos, UK) and AFM (SPM-9600, Shimadazu, Japan).

2.2. Folding and aggregation of GO

GO suspension (1.0 mL, 1.5 mg/mL) was mixed with 1.0 mL deionized water and 1.0 mL $CuCl_2$ (150 mM) by a vortex mixer. The final concentration of the suspension was 500 μg/mL for GO and 50 mM for Cu^{2+}. The GO–Cu^{2+} suspension and GO suspension

(500 μg/mL) were separately placed in vials for photography, and dropped onto glass slides for confocal microscopic observations (FV-1000, Olympus, Japan) under bright field. The suspension was also characterized by SEM (JSM 6700F, Japan), TEM (JEM-200CX, JEOL, Japan) and AFM. In order to investigate the aggregation of GO at single sheet level, highly diluted GO–Cu^{2+} suspension prepared by mixing GO (final concentration of 6 μg/mL) and $CuCl_2$ (final concentration of 150 μM) was examined for the folding of GO by AFM.

As a control, GO (final concentration of 500 μg/mL) was also mixed with NaCl (final concentration of 200 mM) for photographic and confocal microscopic investigations following the same procedures. Highly diluted GO (final concentration of 6 μg/mL) with NaCl (final concentration of 600 μM) was used for the AFM observation.

To demonstrate the coordination of Cu^{2+} by GO, the absorption spectra of GO (500 μg/mL), GO–Cu^{2+} (500 μg/mL GO and 15 mM $CuCl_2$) and $CuCl_2$ (15 mM) at 400–850 nm were recorded.

To re-disperse the GO–Cu^{2+} aggregates, the GO–Cu^{2+} suspension with final concentrations of 500 μg/mL for GO and 50 mM for Cu^{2+} was centrifuged at 14,000 rpm for 30 min and washed by deionized water for five times to remove Cu^{2+}. Next, GO was re-dispersed in deionized water by sonication for 5 min (40 kHz, 50 W). The re-dispersed GO suspension was placed in a vial for photography and dropped on a glass slide for confocal microscopy. Diluted re-dispersed GO suspension was used for the AFM characterization.

2.3. Absorption capacity of GO

The initial pH value of GO and $CuCl_2$ was adjusted to 5.0 with NaOH or HCl aqueous solutions. GO (final concentration of 500 μg/mL) was mixed with $CuCl_2$ in different concentration (final concentrations of 50, 75, 100, 200, 300, 400, 500, 600, 700, 1000 μM). The suspension was fully mixed by a vortex mixer. After mixing under room temperature for 12 h, the mixture was centrifuged at 14,000 rpm for 30 min. The supernatant was taken for Cu^{2+} concentration measurement.

The Cu^{2+} concentration was determined by acetaldehyde–bis(cyclohexanone) oxaldihydrazone (BCO) method [21]. Briefly, 0.7 mL triammonium citrate (20 g triammonium citrate dissolved in 100 mL deionized water), 0.5 mL NH_3–NH_4Cl buffer solution (4 mL $NH_3{\cdot}H_2O$ and 4 g NH_4Cl dissolved in 100 mL deionized water), 0.1 mL acetaldehyde (40%), 1.1 mL BCO (0.2 g dissolved in a mixture of 50 mL deionized water and 50 mL alcohol) and 2.1 mL deionized water were added into 0.5 mL the supernatant solution and mixed by a vortex mixer. After 10 min, the absorbance at 545 nm was recorded. The Cu^{2+} concentration was calculated by referring to the standard curve (Fig. S1). The detection limit of acetaldehyde–BCO method is 0.1 μg/mL, which is lower than the Cu^{2+} concentrations in our experiments.

The obtained equilibrium Cu^{2+} concentration (C_e) and the equilibrium absorption capacity (q_e) values were fitted by Langmuir model and Freundlich model (Eqs. (1) and (2)) [22,23]. The maximum absorption capacity (q_m) was calculated from the Langmuir model for comparison with other absorbents.

$$\frac{1}{q_e} = \frac{1}{q_m} + \frac{1}{bq_mC_e} \quad (1)$$

$$\ln q_e = \ln K_F + \frac{1}{n}\ln C_e \quad (2)$$

3. Results and discussion

3.1. Characterization of GO

GO is prepared following the modified Hummers method and then suspended in water. The AFM investigation suggests that GO in aqueous suspension is mainly in a single-layer state (Fig. 1). The size of GO is in the range of 400 nm–2 μm and the height of GO is around 0.9 nm. Some small wrinkles with heights around 1 nm were also presented under AFM. In the IR spectrum, there is broad absorption at 3400 cm^{-1}, which corresponds to –COOH and –OH groups. The absorption at 1720 cm^{-1} indicates the existence of C=O bonds. The small peaks in the range of 2700–300 cm^{-1} suggest the existence of a few C–H bonds. The peak around 1100 cm^{-1} refers to C–O–C bonds. The observed chemical bonds are all commonly observed in GO samples [16]. The XPS further confirms the existence of oxygen. The oxygen content from XPS is around 36% in mass.

3.2. Folding/aggregation of GO

Upon the addition of Cu^{2+} (final concentration 50 mM, in the form of $CuCl_2$, initial pH 5.0) to the GO suspension (final concentration 500 μg/mL, initial pH 5.0), aggregation took place immediately (Fig. 2). The aggregation is reflected by the increased scattering in the absorption spectra (Figs. 2b and S2). The increased absorption at around 800 nm is assigned to Cu^{2+}. Under optical microscope, the aggregates show ordered, rod-like structure with lengths around 100 μm in suspension (Figs. 2c and S3). The GO sheets are seriously stacked and wrinkled (Stacking refers to parallel packing of GO sheets. Wrinkling refers to a local folding to form wrinkles on a flat GO sheet) in the aggregates (Figs. 2d and S4). It is nearly impossible to distinguish the GO sheets elaborately in the aggregates.

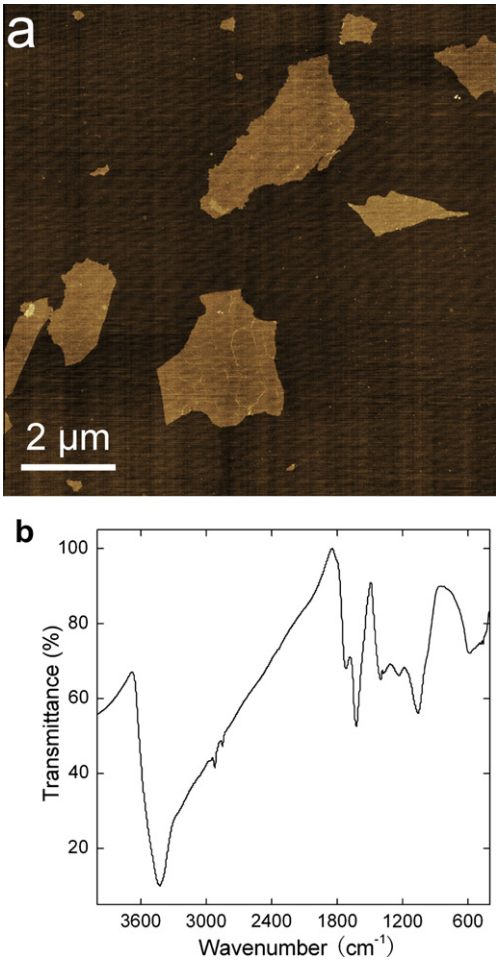

Fig. 1. Representative AFM image (a) and IR spectrum (b) of GO.

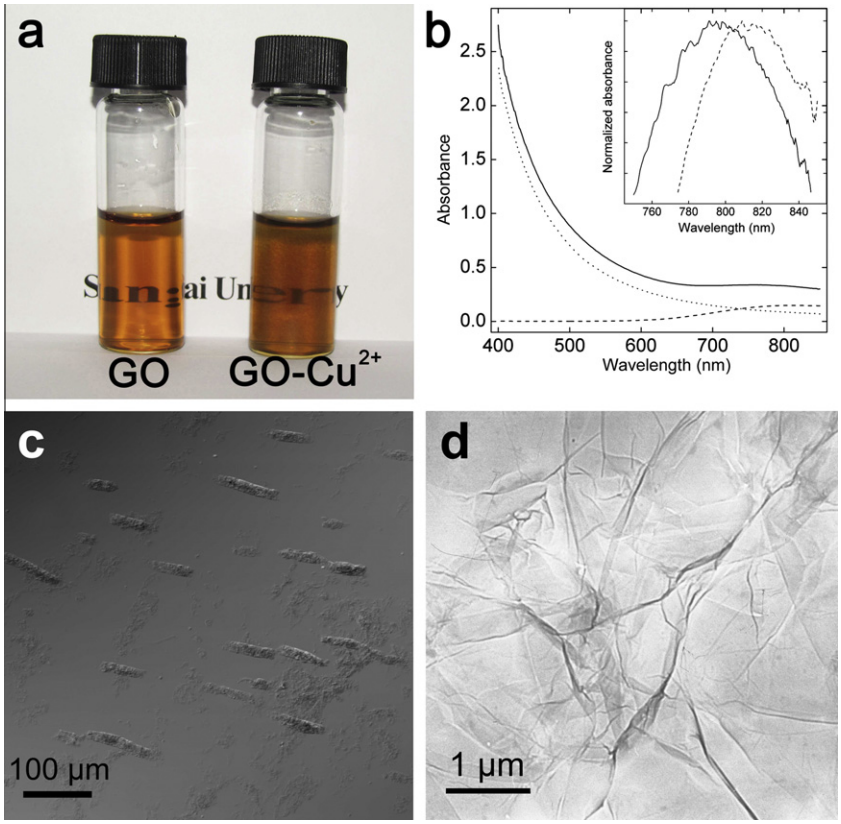

Fig. 2. Aggregation of GO by Cu^{2+}. (a) Photographs of GO and GO–Cu^{2+}; (b) absorption spectra of GO–Cu^{2+} (solid line), GO (dot line) and Cu^{2+} (dash line) and the absorption of Cu^{2+} is featured in the inset; (c) optical microscopic picture of GO–Cu^{2+} aggregates; and (d) TEM image of GO–Cu^{2+} aggregates.

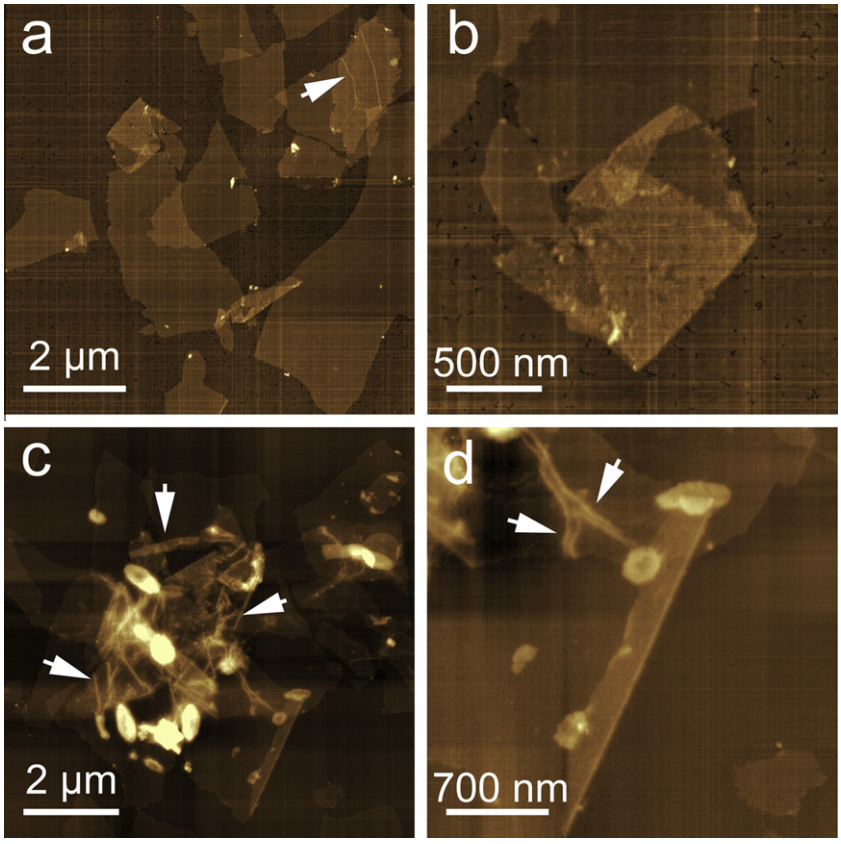

Fig. 3. Representative AFM images of GO upon adding Cu^{2+}. (a) folded GO sheets; (b) zoom in on one folded GO sheet in panel (a); (c) stacked GO sheets; and (d) zoom in on the folded edge of GO sheets in panel (c). The wrinkles are indicated with white arrows.

To investigate the detailed changes upon the addition of Cu^{2+}, highly diluted GO (final concentration of 6 μg/mL) was mixed with excess Cu^{2+} (final concentration of 150 μM) for the AFM investigation (Fig. 3). The folding (refers to a piece of GO sheet bending over to stack with the other part of the same GO sheet) presents in both the stacked GO sheets and individual GO sheets at very low GO concentration. The average distance between the folded layers is around 2 nm, which is higher than the typical single-layer thickness of GO (around 0.9 nm). There are also plenty of wrinkles in the GO sheets. The wrinkles are more than 8 nm in height, much higher than the typical wrinkles in the normal GO (less than 2 nm). Beyond the folding and wrinkling, GO sheets stack with each other, forming large aggregates (over 100 nm in height). The average distance between the stacked sheets varies from 0.9 to 2 nm. It is reasonable that the GO sheets are fluctuant rather than identically flat. At the edge of these large aggregates, we also recognized some folded sheets. It demonstrates that the aggregation is the combined consequence of folding, wrinkling and stacking.

The folding and aggregation of GO should be initially driven by the interaction between GO and Cu^{2+}. The interaction of Cu^{2+} with GO most likely happens at the oxygen sites, because the skeleton carbon has much lower affinity to metal ions than oxygen atoms do [23]. Despite the ambiguity of the structure of GO [16], such interaction might not be surprising, because the absorption of cations by graphite oxide have already been reported in literature [17,24–28]. For example, the strong interaction of oxygen atoms with Cu^{2+} is reported by Xu et al., where the low concentration of Cu^{2+} is adopted to avoid the aggregation and the absorbed Cu^{2+} ions are used as the precursors of Cu_2O nanoparticles [17]. There are two major interactions between GO and Cu^{2+}, namely electrostatic interaction and coordination between Cu^{2+} and carboxyl groups on GO.

Previous reports have suggested that reduced graphene with carboxyl groups can aggregate in the presence of NaCl by electrostatic interaction [29]. However, in our experiment, the control experiment with Na^+ could not induce the aggregation of GO (Fig. 4) at a relative high Na^+ concentration of 200 mM (equivalent ion strength to above 50 mM Cu^{2+}). The GO–Na^+ suspension is just as clear and transparent as GO suspension itself. No GO aggregate could be recognized under optical microscope. Under AFM, most sheets locate separately, though a few of them have slight stacks. Thus, the electrostatic interaction is not the sole driving force for the aggregation of GO. Presumably, at the initial stage, there are other interactions to trigger the aggregation process. The coordination and multi-dentate electrostatic interaction might both contribute to the aggregation.

As for the coordination of Cu^{2+} with oxygen atoms on GO, it is evidenced by the blue shift in the absorption spectra of Cu^{2+}. In the present system, three major ligands are available, namely Cl^-, H_2O and carboxyl groups of GO. The replacement of Cl^- and H_2O by carboxyl groups increases the d orbital splitting energy of Cu^{2+} and consequently causes a blue shift of its absorption spectrum. As shown in Fig. 2c, the spectrum of Cu^{2+} manifests a 20 nm blue shift in the presence of GO. After coordinating with Cu^{2+}, the electrostatic repulsion among the carboxyl groups is reduced significantly [30]. Then, the stacking of GO sheets driven mainly by π–π interactions between carbon skeletons becomes possible [31–33].

As discussed above, the aggregation of GO by means of the metal ions is mainly induced by the interaction between the carboxyl groups on GO and the metal ions. Therefore, other metal ions, which have strong interaction with carboxyl groups, could also induce the similar GO aggregation. For examples, GO can be aggregated by Mg^{2+}, Ca^{2+} and Zn^{2+} following the same procedure.

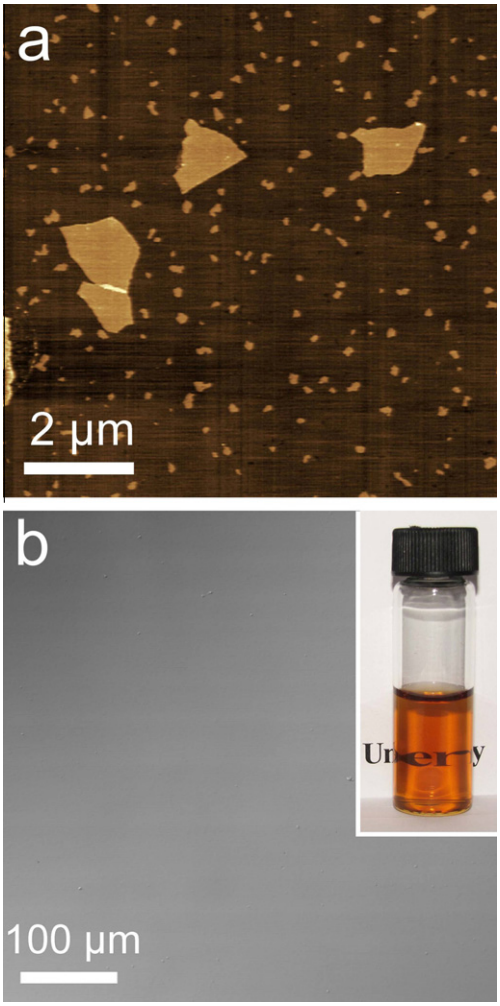

Fig. 4. Characterization of GO upon adding Na^+. (a) representative AFM image and (b) optical microscopic image (inset: photograph).

3.3. Absorption capacity of GO

Beyond the importance from fundamental research aspect, the folding and aggregation of GO may find the potential use in the removal of contaminated Cu^{2+}. We measured the absorption isotherm of Cu^{2+} onto GO to estimate the performance of GO for Cu^{2+} removal. At low C_e values, the q_e values increase sharply (Fig. 5). When C_e is higher than 21.8 mg/L, the absorption capacity approximately reaches a constant value. The clearance ratios are higher than 90% at Cu^{2+} initial concentrations lower than 19.2 mg/L.

The absorption data of GO can be nicely fitted by the Langmuir absorption isotherm model ($R = 0.99$, Fig. 6). The data failed to be fitted by Freundlich model ($R = 0.92$), though it is also widely used in absorption studies. The Langmuir model suggests that Cu^{2+} is absorbed by specific sites of GO and forms monolayer. The q_m is 46.6 mg Cu/g GO, which is much higher than that of carbon nanotubes (CNTs, 28.5 mg Cu/g CNTs) [22] and around 10-fold of that of active carbon (4–5 mg Cu/g active carbon) [34] (measured under the same conditions), ranking it among the most effective absorbents for the Cu^{2+} removal. The performance of GO is also competitive comparing to other Cu^{2+} absorbents, like chitosan, resins, algae and scolecite [35–38]. Because of the different surface and bulk properties, it is very hard to perform a completely fair comparison. Our data provide the useful information at least on the or-

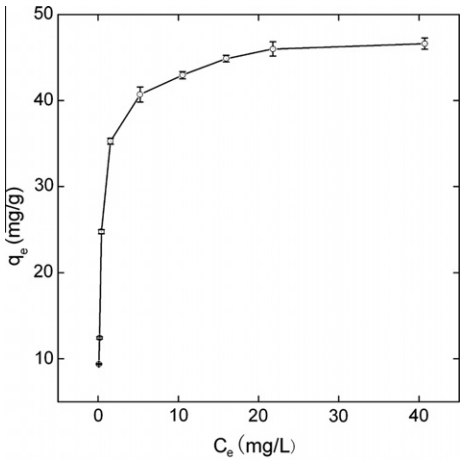

Fig. 5. The absorption isotherm of Cu^{2+} onto GO. Data are presented as the mean of three individual experiments with standard deviation.

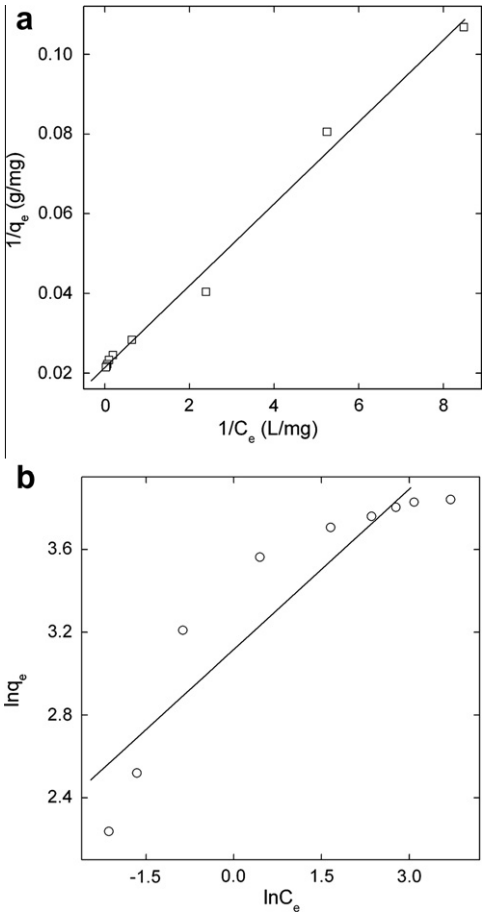

Fig. 6. Langmuir (a) and Freundlich (b) isotherms for the absorption of Cu^{2+} onto GO.

der of magnitude. The huge absorption capacity of GO might owe to the high oxidation degree and large surface of GO. Practically, GO can decrease the Cu^{2+} concentration in water to less than 1.0 mg/L, the recommended Cu^{2+} level for drinking water [39]. Under such condition (C_e = 1.0 mg Cu/L), GO still keeps a high q_e of 31.5 mg Cu/g GO, much more effective than CNTs (22.6 mg Cu/g CNTs) [22]. These results indicate that GO has much stronger binding ability for Cu^{2+} than CNTs do, owing to the strong chelation for Cu^{2+} in the folds and wrinkles of GO.

In addition to its huge Cu^{2+} absorption capacity, the low producing cost of GO could be a vital priority compared with other high performance absorbents. Taking CNTs as an example, previous reports have suggested that CNTs could be used for heavy metal removal [22,40]. However, such application is still on lab research level because of the high producing cost [22,41]. Currently, the absorption behavior of CNTs can only be used in pre-concentration of heavy metals for water analyses [42–44], in which only a small amount of CNTs is required. In contrast, GO can be mass-produced from graphite by simple oxidation reaction using very cheap oxidants. Compared to CNTs, the producing cost of GO is much lower as well as the performance is much higher. Other advantages of Cu^{2+} removal by GO may include the simple separation process of the precipitates and the reversibility of the aggregation (Fig. S5).

4. Conclusions

In summary, the results here demonstrate that Cu^{2+} can induce the folding and aggregation of GO, in which coordination between Cu^{2+} and oxygen atoms on GO is regarded as the primary driving force. The results are highlighted by the excellent Cu^{2+} absorption capacity of GO, ranking GO among the most effective absorbents for Cu^{2+} removal. We believe that our results help to understand the fundamental properties of graphene and represent the great promise of using GO as a Cu^{2+} absorbent.

Acknowledgments

We acknowledge financial support from the China Natural Science Foundation (No. 20871010), the China Ministry of Science and Technology (973 Project Nos. 2006CB705604, 2009CB930200), Shanghai MEC (09YZ16) and Shanghai Leading Academic Disciplines (S30109).

Appendix A. Supplementary material

Supplementary data associated with this article can be found, in the online version, at doi:10.1016/j.jcis.2010.07.042.

References

[1] A.K. Geim, Science 324 (2009) 1530.
[2] C.N.R. Rao, A.K. Sood, K.S. Subrahmanyam, A. Govindaraj, Angew. Chem., Int. Ed. 48 (2009) 7752.
[3] M.J. Allen, V.C. Tung, R.B. Kaner, Chem. Rev. 110 (2010) 132.
[4] A.H.C. Neto, F. Guinea, N.M.R. Peres, K.S. Novoselov, A.K. Geim, Rev. Mod. Phys. 81 (2009) 109.
[5] H.C. Schniepp, K.N. Kudin, J.L. Li, R.K. Prudhomme, R. Car, D.A. Saville, I.A. Aksay, ACS Nano 2 (2008) 2577.
[6] N. Patra, B. Wang, P. Kral, Nano Lett. 9 (2009) 3766.
[7] M.J. Allen, M. Wang, S.A.V. Jannuzzi, Y. Yang, K.L. Wang, R.B. Kaner, Chem. Commun. (2009) 6285.
[8] S. Park, R.S. Ruoff, Nat. Nanotechnol. 4 (2009) 217.
[9] A. Cao, Z. Liu, S. Chu, M. Wu, Z. Ye, Z. Cai, Y. Chang, S. Wang, Q. Gong, Y. Liu, Adv. Mater. 22 (2010) 103.
[10] L. Wang, K. Lee, Y.Y. Sun, M. Lucking, Z. Chen, J.J. Zhao, S.B. Zhang, ACS Nano 3 (2009) 2995.
[11] G.M. Scheuermann, L. Rumi, P. Steurer, W. Bannwarth, R. Mulhaupt, J. Am. Chem. Soc. 131 (2009) 8262.
[12] Z. Liu, J.T. Robinson, X. Sun, H. Dai, J. Am. Chem. Soc. 130 (2008) 10876.
[13] D.A. Dikin, S. Stankovich, E.J. Zimney, R.D. Piner, G.H.B. Dommett, G. Evmenenko, S.T. Nguyen, R.S. Ruoff, Nature 448 (2007) 457.
[14] G. Eda, G. Fanchini, M. Chhowalla, Nat. Nanotechnol. 3 (2008) 270.
[15] X. Wang, L. Zhi, K. Mullen, Nano Lett. 8 (2008) 323.
[16] D.R. Dreyer, S. Park, C.W. Bielawski, R.S. Ruoff, Chem. Soc. Rev. 39 (2010) 228.
[17] C. Xu, X. Wang, L. Yang, Y. Wu, J. Solid State Chem. 182 (2009) 2486.
[18] M. Machida, T. Mochimaru, H. Tatsumoto, Carbon 44 (2006) 2681.
[19] W.S. Hummers Jr, R.E. Offerman, J. Am. Chem. Soc. 80 (1958) 1339.
[20] N.I. Kovtyukhova, P.J. Ollivier, B.R. Martin, T.E. Mallouk, S.A. Chizhik, E.V. Buzaneva, A.D. Gorchinskiy, Chem. Mater. 11 (1999) 771.

[21] A. Wang, X. Huang, J. Mater. Prot. 39 (2006) 73.
[22] Y.H. Li, J. Ding, Z. Luan, Z. Di, Y. Zhu, C. Xu, D. Wu, B. Wei, Carbon 41 (2003) 2787.
[23] M.I. Kandah, J.-L. Meunier, J. Hazard. Mater. 146 (2007) 283.
[24] H.H. Cho, K. Wepasnick, B.A. Smith, F.K. Bangash, D.H. Fairbrother, W.P. Ball, Langmuir 26 (2010) 967.
[25] M. Seredych, T.J. Bandosz, Carbon 45 (2007) 2126.
[26] M. Seredych, T.J. Bandosz, J. Colloid Interface Sci. 324 (2008) 25.
[27] Y. Matsuo, T. Niwa, Y. Sugie, Carbon 37 (1999) 897.
[28] Z. Liu, Z. Wang, X. Yang, K. Ooi, Langmuir 18 (2002) 4926.
[29] D. Li, M.B. Muller, S. Gilje, R.B. Kaner, G.G. Wallace, Nat. Nanotechnol. 3 (2008) 101.
[30] D. Lin, N. Liu, K. Yang, L. Zhu, Y. Xu, B. Xing, Carbon 47 (2009) 2875.
[31] R.J. Chen, Y. Zhang, D. Wang, H. Dai, J. Am. Chem. Soc. 123 (2001) 3838.
[32] S.-T. Yang, H. Wang, L. Guo, Y. Gao, Y. Liu, A. Cao, Nanotechnology 19 (2008) 395101.
[33] F. Lu, X. Wang, M.J. Meziani, L. Cao, L. Tian, M.A. Bloodgood, J. Robinson, Y.-P. Sun, Langmuir 26 (2010) 7561.
[34] H.K. An, B.Y. Park, D.S. Kim, Water Res. 35 (2001) 3551.
[35] W.S.W. Ngah, I.M. Isa, J. Appl. Polym. Sci. 67 (1998) 1067.
[36] O. Hamdaoui, J. Hazard. Mater. 161 (2009) 737.
[37] Q. Yu, J.T. Matheickal, P. Yin, P. Kaewsarn, Water Res. 33 (1999) 1534.
[38] S.T. Bosso, J. Enzweiler, Water Res. 336 (2002) 4795.
[39] United States Environmental Protection Agency, National Primary Drinking Water Regulations (EPA 816-F-09-004), EPA, Washington, 2009.
[40] G.P. Rao, C. Lu, F. Su, Sep. Purif. Technol. 58 (2007) 224.
[41] C. Lu, C. Liu, G.P. Rao, J. Hazard. Mater. 151 (2008) 239.
[42] M. Tuzen, K.O. Saygi, M. Soylak, J. Hazard. Mater. 152 (2008) 632.
[43] T. Shamspur, A. Mostafavi, J. Hazard. Mater. 168 (2009) 1548.
[44] Z. Zang, Z. Hu, Z. Li, Q. He, X. Chan, J. Hazard. Mater. 172 (2009) 958.